Journal of Industrial and Engineering Chemistry 18 (2012) 1925–1930

Contents lists available at SciVerse ScienceDirect

Journal of Industrial and Engineering Chemistry

journal homepage: www.elsevier.com/locate/jiec

Preparation of bionanoparticles derived from *Spirulina platensis* and its application for Cr (VI) removal from aqueous solutions

G.L. Dotto, T.R.S. Cadaval, L.A.A. Pinto *

Unit Operation Laboratory, School of Chemistry and Food, Federal University of Rio Grande – FURG, 475 Engenheiro Alfredo Huch Street, 96203-900 Rio Grande, RS, Brazil

ARTICLE INFO

Article history:
Received 6 April 2012
Accepted 10 May 2012
Available online 18 May 2012

Keywords:
Biosorbent
Ion removal
Nanoparticles
Polydispersity index

ABSTRACT

Spirulina platensis nanoparticles were prepared by mechanical agitation and were applied to removal Cr (VI) from aqueous solutions. Nanoparticles preparation was function of stirring rate and contact time. In the optimal conditions, Cr (VI) removal by nanoparticles as a function of pH and initial ion concentration was carried out. The optimal conditions for preparation were 10,000 rpm and 20 min, and the nanoparticles presented mean diameter of 215.6 nm and polydispersity index of 0.151. The best conditions for Cr (VI) removal were at pH 4 and ion concentration of 250 mg L^{-1}, and the Cr (VI) removal percentage was 99.1%.

1. Introduction

Spirulina platensis biomass has been used as a promising biosorbent to removal heavy metals from aqueous solutions [1–9]. *S. platensis* is a planktonic photosynthetic filamentous cyanobacterium that forms massive populations in tropical and subtropical bodies of water, and it is identified by the main morphological arrangement of multicellular cylindrical trichomes in a helix along the entire length of the filaments [10,11]. Its biomass contains a variety of biomolecules and functional groups which can be responsible for pollutants binding [1,2,12]. However, all properties of *S. platensis* are not accessible in the natural form of the biomass [8,12], thus, the preparation of the nanoparticles from biomass is an alternative to improve the applicability of *S. platensis*.

Nanoparticles are defined as particulate dispersions or solid particles with a size in the range of 1–1000 nm [13,14]. The methods used to produce nanoparticles can be divided into three main groups: (i) physicochemical methods, (ii) in situ chemical synthesis methods and (iii) mechanical methods [15]. The mechanical agitation method is a fast and simple way to obtain nanoparticles, due its easy of application and use of few chemical reagents [13,14]. Due to their unique physical and chemical properties, especially their small particle size, nanoparticles has been used to removal pollutants from aqueous solutions [12,16–18], but nanoparticles from microalgae biomass are rarely investigated [12].

Metals are a major category of globally-distributed pollutants and many of them are toxic at very low concentration [19–21]. Hexavalent chromium (Cr (VI)) is considered as a major pollutant in water pollution and has a dominant presence in most of the effluent streams [22]. Several industries like paint and pigment manufacturing, stainless steel production, corrosion control, leather tanning, chromium plating, wood preservation, fertilizers, textile, photography and others, discharge effluent containing Cr (VI) to surface water [19,23–25]. The concentration of Cr (VI) present in industrial effluent streams are in the range of 50–200 mg L^{-1} and the tolerance limit for discharge into inland surface waters is 0.1 mg L^{-1} [23]. Its permissible limit in potable water is 0.05 mg L^{-1} [22]. Conventional methods applied for Cr (VI) removal are mainly chemical precipitation, oxidation/reduction, filtration, ion exchange, membrane separation and adsorption [24]. Alternatively to these methods, the biosorption of heavy metals by algal biomass has been successfully used [1–9,19,25,26].

This work aimed to prepare *S. platensis* nanoparticles for Cr (VI) removal from aqueous solutions. The preparation of the nanoparticles was optimized as a function of stirring rate (3000–17,000 rpm) and contact time (6–34 min) by a central composite design. The responses were the mean diameter and polydispersity index of the nanoparticles. In the best conditions, the nanoparticles were employed to removal Cr (VI) from aqueous solutions. The Cr (VI) removal by *S. platensis* nanoparticles was optimized as a function of pH (4–8) and initial ion concentration (50–250 mg L^{-1}) using a full factorial design.

* Corresponding author. Tel.: +55 53 3233 8645; fax: +55 53 3233 8745.
E-mail addresses: guilherme_dotto@yahoo.com.br (G.L. Dotto), titoeq@gmail.com (T.R.S. Cadaval), dqmpinto@furg.br (L.A.A. Pinto).

1226-086X/$ – see front matter © 2012 The Korean Society of Industrial and Engineering Chemistry. Published by Elsevier B.V. All rights reserved.
http://dx.doi.org/10.1016/j.jiec.2012.05.005

2. Materials and methods

2.1. Culture conditions and drying of S. platensis

S. platensis strain LEB-52 was cultivated in a 450 L open outdoor photo-bioreactors, under uncontrolled conditions, in the south of Brazil. During these cultivations, water was supplemented with 20% Zarrouk synthetic medium containing (g L^{-1}): $NaHCO_3$, 16.8; $NaNO_3$, 2.5; K_2HPO_4, 0.5; K_2SO_4, 1.0; NaCl, 1.0; $MgSO_4{\cdot}7H_2O$, 0.2; $CaCl_2$, 0.04; $FeSO_4{\cdot}7H_2O$, 0.01; EDTA, 0.08 and micronutrients [27]. At the end of cultivation, the biomass was recovered by filtration, washed with distilled water and pressed to recover the biomass with a moisture content of 76.0% (wet basis).

The wet biomass was dried at 60 °C by a perforated tray drier with perpendicular air flow according to Oliveira et al. [28].

2.2. Preparation and characterization of S. platensis nanoparticles

The nanoparticles were obtained from *S. platensis* biomass through a mechanical agitation method [12–15]. Firstly, the dried biomass was ground by a mill (Wiley Mill Standard, No. 03, USA) and it was sieved until the discrete particle size ranged from 68 to 75 μm. The sieved biomass (100 mg) was added in distilled water (40 mL) and the pH was adjusted using 10 mL of a buffer disodium phosphate/citric acid solution (0.1 mol L^{-1}). After, the suspensions were agitated (Dremel, 1100-01, Brazil) at different time intervals. Preliminary tests showed that the mean diameter and polydispersity index of the nanoparticles were not influenced in the pH range from 2 to 8. In the same way, amounts of sieved biomass ranged from 20 to 500 mg found similar results. The experimental runs were carried out in replicate ($n = 2$) at ambient temperature (25 ± 1 °C).

The mean diameter and polydispersity index of the nanoparticles were obtained by dynamic light scattering (DLS) [29]. The dynamic light scattering equipment was constituted by a laser (Spectra-physics, 127, USA) coupled to a goniometer (Brookheaven, BI-200M, USA) and a digital correlator (Brookheaven, BI-9000AT, USA). The DLS measures Brownian motion and relates this to the size of the particles [30]. In this work, the hydrodynamic diameter or mean diameter was calculated from the translational diffusion coefficient by using the Stokes–Einstein equation [29,30], as presented in Eq. (1):

$$D_t = \frac{TK_B}{3\pi\eta d} \quad (1)$$

where "d" is the hydrodynamic diameter (m), D_t is the translational diffusion coefficient ($m^2\ s^{-1}$), K_B is Boltzmann's constant, T is the absolute temperature (K) and η is the viscosity ($kg\ m^{-1}\ s^{-1}$).

A central composite design (2^2 with three central and four axial points) was utilized to study the preparation of the nanoparticles [31]. The effects of stirring rate (3000–17,000 rpm) and contact time (6–34 min) on the mean diameter (D) and polydispersity index (PDI) of the nanoparticles were evaluated. The factors and levels were determined by preliminary tests and its values are shown in Table 1.

The responses (D and PDI) were represented as a function of independent variables, according to a quadratic polynomial equation, Eq. (2):

$$Y = a + \sum_{i=1}^{3} b_i x_i + \sum_{i=1}^{3} b_{ii} x_i^2 + \sum_{i=1}^{2} \sum_{j=i+1}^{3} b_{ij} x_i x_j \quad (2)$$

where "Y" is the predicted response (D or PDI), "a" the constant coefficient, b_i the linear coefficients, b_{ij} the interaction coefficients, b_{ii} the quadratic coefficients, x_i and x_j are the coded values of the variables.

The statistical significance of the nonlinear regression was determined by Student's test. The second order model was evaluated by Fischer's test and the proportion of variance explained by the model obtained was given by the coefficient of determination, R^2. Experimental runs were performed at random and the results were analyzed by Statistica version 7 (StatSoft Inc., USA) software.

In the best conditions (obtained from the central composite design), the *S. platensis* nanoparticles were characterized by scanning electron microscopy (SEM) (Jeol, JSM-6060, Japan) [13] and energy dispersive X-ray spectroscopy (EDS) (Jeol, JSM-5800, Japan) [12].

2.3. Studies of Cr (VI) removal

S. platensis nanoparticles obtained in the best conditions were employed for Cr (VI) removal from aqueous solutions by batch studies. Stock Cr (VI) solution of 1.0 g L^{-1} was prepared by $K_2Cr_2O_7$ in distilled water. The batch experiments were carried out in erlenmeyer flasks at 298 K, under constant agitation of 100 rpm (Nova Ética, 109-1, Brazil). Firstly, 40 mL of a suspension containing 100 mg of nanoparticles had the pH corrected (pH 4, 6 and 8) through the 10 mL of buffer disodium phosphate/citric acid solution (0.1 mol L^{-1}). After, 50 mL of Cr (VI) solutions with different concentrations were added in these suspensions in order to obtain initial Cr (VI) concentrations of 50, 150 and 250 mg L^{-1}. This manner the initial concentration of *S. platensis* nanoparticles was 1.0 g L^{-1}. The erlenmeyer flasks were agitated until the equilibrium and the Cr (VI) concentration was determined by spectrophotometry (Quimis, Q108, Brazil) at 540 nm using 1,5-diphenyl carbazide as the complexing agent [24]. The experimental runs were carried out in replicate (three times for each experiment) and blanks (suspensions containing 1 g L^{-1} of *S. platensis* nanoparticles and buffer) were performed. The Cr (VI)

Table 1
Experimental conditions and responses (mean diameter and polydispersity index) for the preparation of the *S. platensis* nanoparticles according to the matrix of central composite design.

Experiment (no.)	Stirring rate (rpm)	Contact time (min)	Mean diameter (D) (nm)[a]	Polydispersity index (PDI)[a]
1	15,000	30	435.0 ± 2.1	0.151 ± 0.001
2	15,000	10	354.5 ± 1.7	0.175 ± 0.001
3	5000	30	566.5 ± 2.0	0.647 ± 0.007
4	5000	10	652.5 ± 1.9	0.545 ± 0.005
5	17,000	20	532.1 ± 2.5	0.145 ± 0.001
6	3000	20	653.8 ± 1.0	0.858 ± 0.004
7	10,000	34	545.7 ± 1.3	0.346 ± 0.003
8	10,000	6	451.8 ± 0.9	0.213 ± 0.001
9	10,000	20	213.4 ± 1.0	0.150 ± 0.002
10	10,000	20	215.0 ± 0.9	0.150 ± 0.002
11	10,000	20	217.8 ± 1.2	0.152 ± 0.001

[a] Mean ± standard error ($n = 2$).

Table 2
Experimental conditions and Cr (VI) removal percentage (R) according to the matrix of 3^2 full factorial design.

Experiment (no.)	pH	Cr (VI) initial concentration (mg L^{-1})	Cr (VI) removal percentage (R) (%)[a]
1	4	50	78.7 ± 1.5
2	4	150	90.9 ± 1.6
3	4	250	97.5 ± 0.9
4	6	50	59.6 ± 2.0
5	6	150	71.7 ± 1.3
6	6	250	82.6 ± 0.5
7	8	50	26.4 ± 1.0
8	8	150	35.3 ± 0.2
9	8	250	37.2 ± 0.8

[a] Mean ± standard error (n = 3).

removal percentage (R) was calculated by Eq. (3):

$$R\,(\%) = \frac{C_0 - C_e}{C_0} 100 \quad (3)$$

where C_0 and C_e are the initial and equilibrium concentrations of Cr (VI) in liquid phase (mg L^{-1}).

A full factorial design 3^2 was used to optimize the Cr (VI) removal by *S. platensis* nanoparticles as a function of pH (4–8) and Cr (VI) initial concentration (50–250 mg L^{-1}) [31]. Table 2 shows the factors and the levels of the full factorial design, and its values were determined by the literature [1–9,17,18,22–25] and preliminary tests. The response was the Cr (VI) removal percentage (R), which was represented as a function of independent variables, according a quadratic polynomial equation similar to Eq. (2). The statistic treatment was similar to Section 2.2.

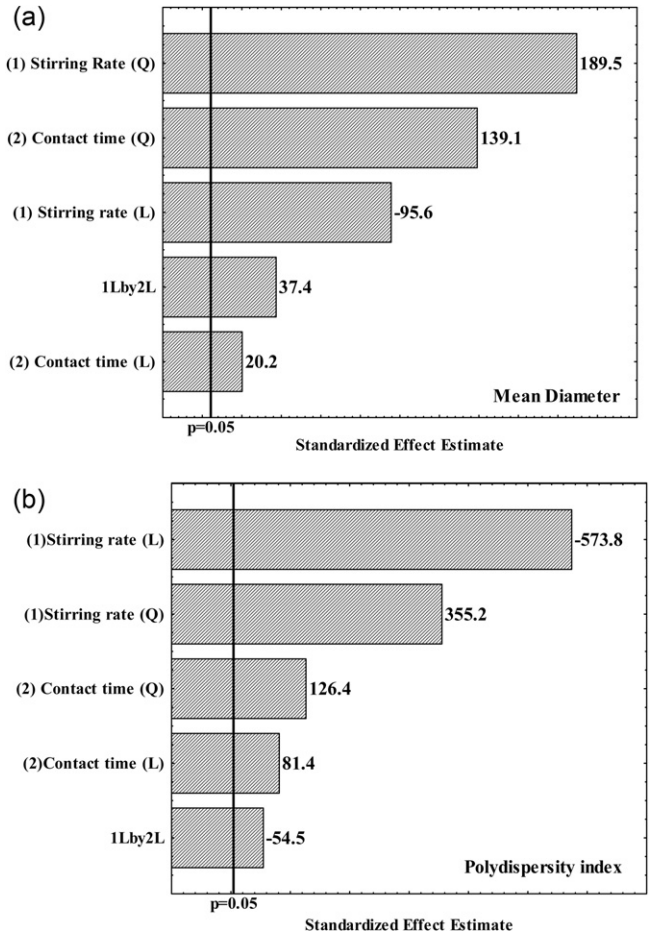

Fig. 1. Pareto charts of (a) mean diameter (D) and (b) polydispersity index (PDI).

3. Results and discussion

3.1. Optimization of S. platensis nanoparticles preparation

Pareto charts were obtained by statistical analysis from the results according to the central composite design shown in Table 1 in order to verify the significance of stirring rate, contact time and its interaction on the mean diameter and polydispersity index of the nanoparticles. Pareto charts, for mean diameter and polydispersity index are shown in Fig. 1.

It was observed that for the mean diameter (Fig. 1(a)) and for the polydispersity index (Fig. 1(b)), all the linear and quadratic main effects and the interaction effect were significant ($p \leq 0.05$). Eqs. (4) and (5) show, respectively, the mean diameter (D) and the polydispersity index (PDI) as a function of stirring rate (x_1) and contact time (x_2).

$$D = 215.6 + 178.3x_1^2 + 130.9x_2^2 - 75.4x_1 + 15.9x_2 + 41.6x_1x_2 \quad (4)$$

$$PDI = 0.151 + 0.173x_1^2 + 0.062x_2^2 - 0.235x_1 + 0.033x_2 - 0.031x_1x_2 \quad (5)$$

In order to verify the prediction and significance of the models (Eqs. (4) and (5)), analysis of variance and Fischer F-test were employed. It was observed that the mean diameter model (Eq. (4)) was significant and predictive, because calculated Fischer, (F_{calc} = 10.98) was about two times superior in relation to standard Fischer (F_{std} = 5.05) and the coefficient of determination R^2 = 0.95. In the same way, polydispersity index model (Eq. (5)) was significant and predictive, (F_{calc} = 83.33) was about fifteen times superior in relation to (F_{std} = 5.05) and coefficient of determination R^2 = 0.98. In this way, response surfaces based in the models were used to represent the mean diameter and the polydispersity index of the nanoparticles as a function of independent variables. Fig. 2 shows response surfaces of the mean diameter (a) and of polydispersity index (b).

It was observed in Fig. 2 that the stirring rate effect was different for each response (mean diameter and polydispersity index). Fig. 2(a) shows that the mean diameter of the nanoparticles presented a parabolic behavior in relation to stirring rate, being the lower values obtained at 10,000 rpm. On the other hand, a decrease in the polydispersity index was observed until 15,000 rpm (Fig. 2(b)), above this, a little variation was observed. This can be occurred because, the stirring rate increase until 10,000 rpm, caused an increase in the energy dissipation and turbulence in the mixing zone, leading to a break-up of larger *S. platensis* particles into smaller nanoparticles. Above 10,000 rpm, it can be inferred that the formation of aggregates occurred, increasing the mean diameter of the nanoparticles. According to Fan et al. [32], intense stirring may destroy the repulsive force between the particles and lead to an aggregation. Similar behavior was obtained by

Salimi et al. [33] in the preparation of hydroxyapatite nanoparticles. They showed that a stirring rate increase until 3000 rpm caused a decrease in particle size, but, a new increase to 7000 rpm had no effect. Javadzadeh et al. [34] studied stirring rate in the range from 10,000 to 20,000 rpm in the preparation of naproxen–PLGA nanoparticles, and they found lower *PDI* values at 20,000 rpm, and the nanoparticles were monodisperse in all conditions.

The contact time effect was the same for mean diameter (Fig. 2(a)) and polydispersity index (Fig. 2(b)) of the *S. platensis* nanoparticles. It was observed a parabolic behavior with a minimum point at 20 min. This shows that an increase in contact time until 20 min cause a decrease in the mean diameter (*D*) and polydispersity index (*PDI*), but, *D* and *PDI* are increased when the contact time is increased from 20 to 34 min. On the basis in these results, it can be inferred that the break of the particles occurred until 20 min, and after this time, kinetic coagulation occurred, leading to a formation of stable aggregates, and consequently, increasing the mean diameter and polydispersity index of the *S. platensis* nanoparticles. According to Salimi et al. [33], the kinetic coagulation can lead to the formation of stable aggregates increasing the mean diameter of the nanoparticles.

The optimal conditions for the preparation of the *S. platensis* nanoparticles were obtained by determining the minimum point of the response surfaces (Fig. 2), being, 10,000 rpm and 20 min for the mean diameter, and 15,000 rpm and 20 min for the polydispersity index. Despite 15,000 rpm provide the lower value of *PDI*, the use of 10,000 rpm also provides monodisperse nanoparticles. This manner, in the experimental range, the optimal conditions were: 10,000 rpm and 20 min. In these conditions, the mean diameter (*D*) and the polydispersity index (*PDI*) of the *S. platensis* nanoparticles were, respectively, 215.6 nm and 0.151. Javadzadeh et al. [34] obtained naproxen–PLGA nanoparticles in the range from 352 to 571 nm with *PDI* of 0.16–0.36, by a single emulsion technique. Adibkia et al. [35] obtained monodisperse Naproxen-eudragit® RS100 nanoparticles (*PDI* 0.12–0.29) in the range from 378 to 644 nm.

Fig. 3 shows, respectively, (a) the SEM image and (b) the EDS spectrum of the *S. platensis* nanoparticles obtained in the best condition. In Fig. 3(a) it can be observed that *S. platensis* nanoparticles were homogeneous, showing an ellipsoidal–spherical form and a uniform size distribution. In EDS analysis (Fig. 3(b)), it was observed that the major elements on the surface of *S. platensis* nanoparticles were C (55%), N (32%), O (10%), P (2%) and S (1%).

3.2. Application of S. platensis nanoparticles for Cr (VI) removal

S. platensis nanoparticles obtained in the optimal conditions (10,000 rpm and 20 min) were employed to Cr (VI) removal from aqueous solutions. Pareto chart was generated by statistical analysis from the results (Table 2) in order to verify the significance of pH and Cr (VI) initial concentration on the Cr (VI) removal percentage (*R*). Fig. 4 shows the Pareto chart of Cr (VI) removal percentage (*R*).

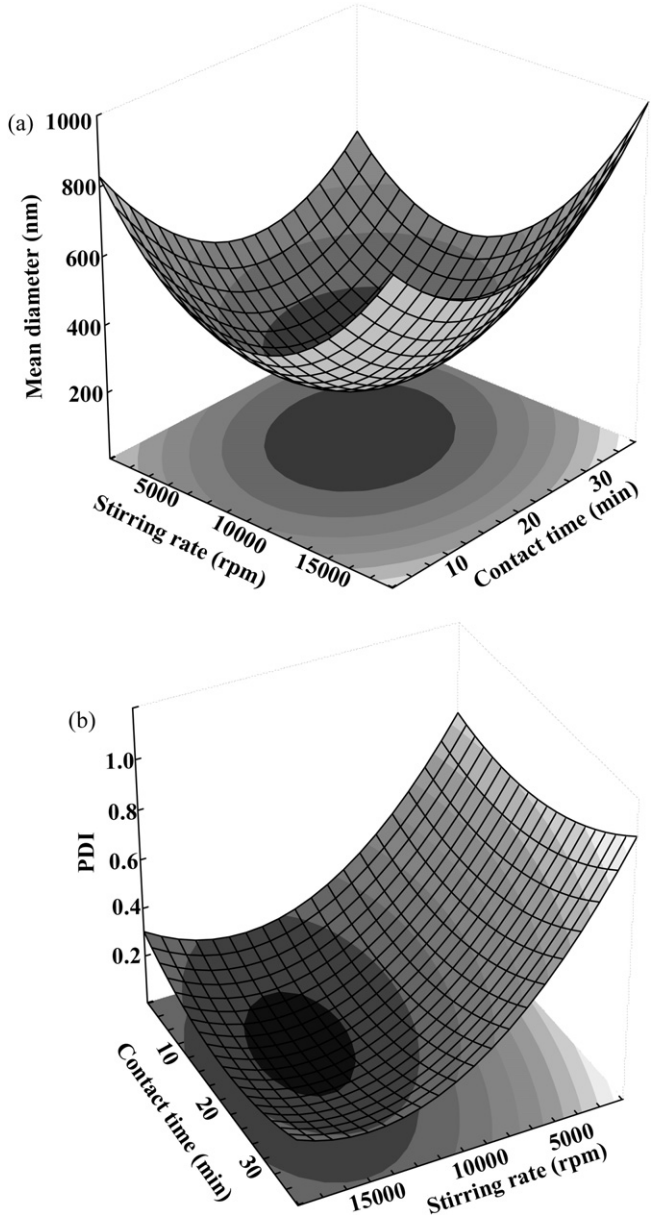

Fig. 2. Response surfaces of (a) mean diameter (*D*) and (b) polydispersity index (*PDI*) as a function of stirring rate and contact time.

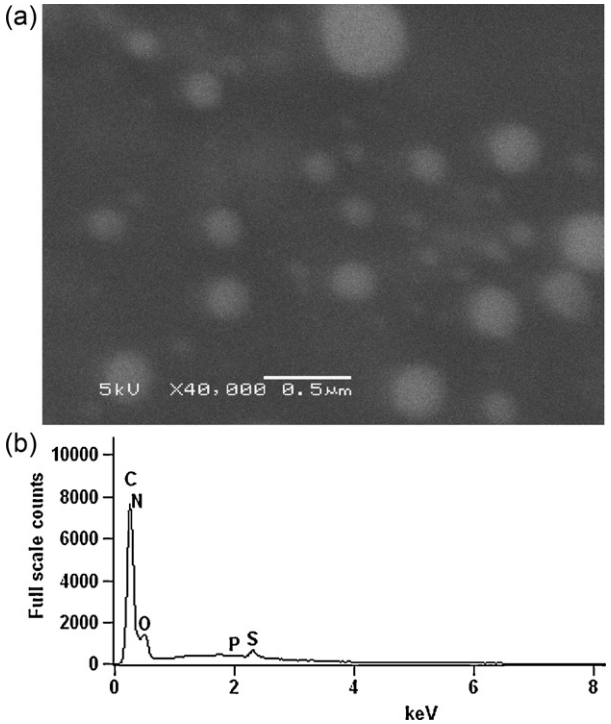

Fig. 3. Characteristics of *S. platensis* nanoparticles: (a) SEM image and (b) EDS spectrum.

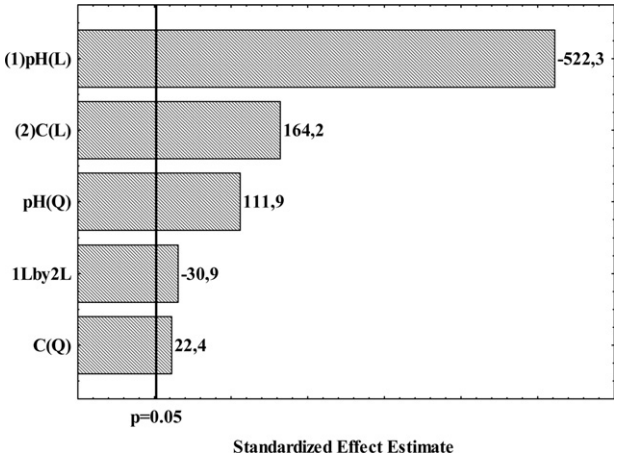

Fig. 4. Pareto chart of Cr (VI) removal percentage (R).

As can be seen in Fig. 4, all linear and quadratic main effects were significant in relation to the Cr (VI) removal percentage ($p \leq 0.05$). The interaction effect was also significant ($p \leq 0.05$). Eq. (6) shows the Cr (VI) removal percentage (R) as a function of pH (y_1) and Cr (VI) initial concentration (y_2).

$$R\,(\%) = 72.7 - 10.4y_1^2 - 2.1y_2^2 - 27.9y_1 + 8.8y_2 - 2.0y_1y_2 \qquad (6)$$

From the statistical treatment (similar to the Section 3.1), it was verified that the Cr (VI) removal percentage model (Eq. (6)) was significant ($R^2 = 0.99$) and predictive (calculated Fischer ($F_{calc} = 531.73$) was about a hundred times superior in relation to standard Fischer ($F_{std} = 5.06$)). This manner, the Cr (VI) removal percentage (R) was represented as a function of the independent variables by a response surface. Fig. 5 shows the response surface of Cr (VI) removal percentage (R) as a function of pH and Cr (VI) initial concentration.

It can be observed in Fig. 5 that the Cr (VI) removal percentage was increased with the pH decrease, reaching maximum values at pH 4. This behavior can be explained as follows: Under acid conditions, different species of Cr (VI) ($Cr_2O_7^{2-}$, $HCrO_4^-$, $Cr_3O_{10}^{2-}$, $Cr_4O_{13}^{2-}$) coexist [17], and the dominant form at pH 4.0 is the acid chromate ion species ($HCrO_4^-$) [23]. Coupled to this, the *S. platensis*

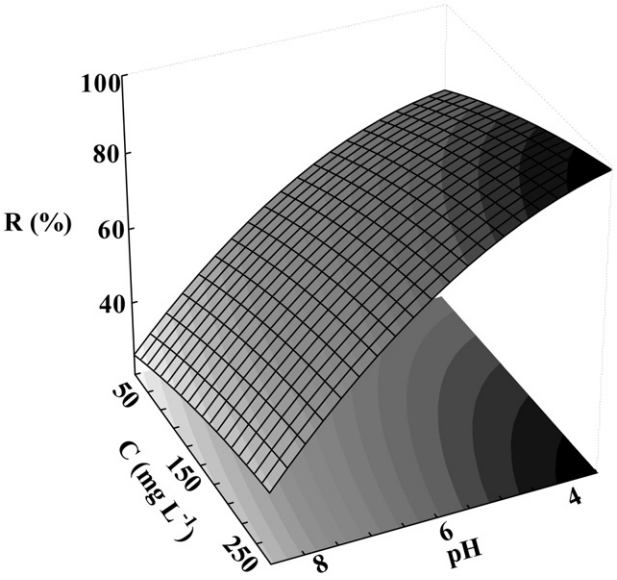

Fig. 5. Response surface of Cr (VI) removal percentage (R) as a function of pH and initial concentration.

Table 3
Comparison between *S. platensis* nanoparticles and others adsorbents to removal Cr (VI).

Adsorbent	Cr (VI) removal percentage (%)	Reference
S. platensis nanoparticles	99.1	This work
Immobilized *S. platensis* in calcium alginate	99.0	[5]
Diatomite-supported/unsupported magnetite nanoparticles	99.8	[17]
Sawdust	74.6	[22]
Activated carbon derived from olive bagasse	97.0	[23]
Chitosan	92.9	[24]
Dolomite	≈95.0	[36]
Coir pith	94.0	[37]
Sand coated with Fe and Mn oxides	≈20.0	[38]

nanoparticles are positively charged at pH values below 7.0 [12]. This manner, at low values of pH, electrostatic attractions can occur between the positively charged *S. platensis* nanoparticles and the Cr (VI) species negatively charged, increasing the Cr (VI) removal percentage. On the other hand, *S. platensis* nanoparticles are negatively charged at pH values above 7.0 [12]. Thus, at high pH values, the Cr (VI) removal percentage decreases due to the repulsion between negatively charged chromium ions and *S. platensis* nanoparticles. According to Albadarin et al. [36] this indicates that ion exchange and electrostatic interactions can be involved in the interaction mechanism. This behavior was also observed by others researchers [17,18,36].

Fig. 5 shows that the Cr (VI) removal percentage was favored by the increase in Cr (VI) initial concentration. This can be attributed to the increase in concentration gradient in the system which results with enhanced efficiency of Cr (VI) removal [24]. Similar behavior was obtained by Sumathi et al. [37] in the adsorption of Cr (VI) onto charcoal. In their work, the increase in Cr (VI) initial concentration from 20 to 100 mg L^{-1} caused an increase in removal percentage from 5 to 45%.

The optimal condition for Cr (VI) removal by *S. platensis* nanoparticles was obtained by the maximum point of the response surface (Fig. 5), being this in pH value of 4 and initial concentration of 250 mg L^{-1}. Under this condition, the Cr (VI) removal percentage was 99.1%. The potential of *S. platensis* nanoparticles for Cr (VI) removal was compared with other adsorbents, as presented in Table 3. This table shows that the *S. platensis* nanoparticles is an alternative biosorbent to removal Cr (VI) from aqueous solutions.

4. Conclusion

S. platensis nanoparticles were prepared by a mechanical agitation method and the preparation was optimized as a function of stirring rate and contact time. The best conditions were 10,000 rpm and 20 min. In these conditions, ellipsoidal–spherical and monodisperse nanoparticles with mean diameter of 215.6 nm and polydispersity index of 0.151 were obtained.

The nanoparticles ($D = 215.6$ nm and $PDI = 0.151$) were employed to removal Cr (VI) from aqueous solutions. The Cr (VI) removal by *S. platensis* nanoparticles was optimized as a function of pH and Cr (VI) initial concentration. The best conditions were pH value of 4 and initial ion concentration of 250 mg L^{-1}. In these conditions, the Cr (VI) removal percentage was 99.1%. These results show that the *S. platensis* nanoparticles can be alternatively used to removal Cr (VI) from aqueous solutions.

Acknowledgments

The authors would like to thank CAPES (Coordination of Improvement of Higher Education Personnel) and CNPq (National

Council of Scientific and Technological Development) for the financial support.

References

[1] A. Çelekli, H. Bozkurt, Desalination 275 (2011) 141.
[2] A. Çelekli, M. Yavuzatmaca, H. Bozkurt, Journal of Hazardous Materials 173 (2010) 123.
[3] C. Solisio, A. Lodi, D. Soletto, A. Converti, Bioresource Technology 99 (2008) 5933.
[4] A. Lodi, D. Soletto, C. Solisio, A. Converti, Chemical Engineering Journal 136 (2008) 151.
[5] S.V. Gokhale, K.K. Jyoti, S.S. Lele, Journal of Hazardous Materials 170 (2009) 735.
[6] A. Şeker, T. Shahwan, A.E. Er?glu, S. Yılmaz, Z. Demirel, M.C. Dalay, Journal of Hazardous Materials 154 (2008) 973.
[7] K. Chojnacka, A. Chojnacki, H. Gorecka, Chemosphere 59 (2005) 75.
[8] R. Gong, Y. Ding, H. Liu, Q. Chen, Z. Liu, Chemosphere 58 (2005) 125.
[9] L. Fang, C. Zhou, P. Cai, W. Chen, X. Rong, K. Dai, W. Liang, J.D. Gu, Q. Huang, Journal of Hazardous Materials 190 (2011) 810.
[10] M.A. Borowitzka, L.J. Borowitzka, Microalgal Biotechnology, Cambridge University Press, London, 1992.
[11] A. Vonshak, *Spirulina platensis* (Arthrospira): Physiology, Cell-Biology and Biotechnology, Taylor and Francis, London, 1997.
[12] G.L. Dotto, E.C. Lima, L.A.A. Pinto, Bioresource Technology 103 (2012) 123.
[13] X. Li, N. Anton, C. Arpagaus, F. Belleteix, T.F. Vandamme, Journal of Controlled Release 147 (2010) 304.
[14] N. Anton, J.P. Benoit, P. Saulnier, Journal of Controlled Release 128 (2008) 185.
[15] L.M. Zhao, L.E. Shi, Z.L. Zhang, J.M. Chen, D.D. Shi, J. Yang, Z.X. Tang, Brazilian Journal of Chemical Engineering 28 (2011) 353.
[16] T. Basu, U.C. Ghosh, Journal of Industrial and Engineering Chemistry 17 (2011) 834.
[17] P. Yuan, D. Liu, M. Fan, D. Yang, R. Zhu, F. Ge, J.X. Zhu, H. He, Journal of Hazardous Materials 173 (2010) 614.
[18] B. Geng, Z. Jin, T. Li, X. Qi, Chemosphere 75 (2009) 825.
[19] F. Fu, Q. Wang, Journal of Environmental Management 92 (2011) 407.
[20] M. Ahmad, A.R.A. Usman, S.S. Lee, S.C. Kim, J.H. Joo, J.E. Yang, Y.S. Ok, Journal of Industrial and Engineering Chemistry 18 (2012) 198.
[21] G. Blázquez, M.A. Martín-Lara, E. Dionisio-Ruiz, G. Tenorio, M. Calero, Journal of Industrial and Engineering Chemistry 17 (2011) 824.
[22] S. Gupta, B.V. Babu, Bioresource Technology 100 (2009) 5633.
[23] H. Demiral, I. Demiral, F. Tumsek, B. Karabacak?glu, Chemical Engineering Journal 144 (2008) 188.
[24] Y.A. Aydin, N.D. Aksoy, Chemical Engineering Journal 151 (2009) 188.
[25] M. López-García, P. Lodeiro, R. Herrero, M.E.S. de Vicente, Journal of Industrial and Engineering Chemistry (2012), http://dx.doi.org/10.1016/j.jiec.2012.01.036.
[26] Z. Aksu, Process Biochemistry 40 (2005) 997.
[27] J.A.V. Costa, L.M. Colla, P.F.F. Duarte, Bioresource Technology 92 (2004) 237.
[28] E.G. Oliveira, G.S. Rosa, M.A. Moraes, L.A.A. Pinto, Bioresource Technology 100 (2009) 1297.
[29] J. Bruce, R. Pecora, Dynamic Light Scattering: With Applications to Chemistry, Biology and Physics, Dover Publications, New York, 2000.
[30] S.K. Brar, M. Verma, Trends in Analytical Chemistry 30 (2011) 4.
[31] R.H. Myers, D.C. Montgomery, Response Surface Methodology: Process and Product Optimization Using Designed Experiments, John Wiley & Sons, New York, 2002.
[32] W. Fan, W. Yan, Z. Xu, H. Ni, Colloids and Surfaces B: Biointerfaces 90 (2012) 21.
[33] M.N. Salimi, R.H. Bridson, L.M. Grover, G.A. Leeke, Powder Technology 218 (2012) 109.
[34] Y. Javadzadeh, F. Ahadi, S. Davaran, G. Mohammadi, A. Sabzevari, K. Adibkia, Colloids and Surfaces B: Biointerfaces 81 (2010) 498.
[35] K. Adibkia, Y. Javadzadeh, S. Dastmalchi, G. Mohammadi, F.K. Niri, M.A. Beiram, Colloids and Surfaces B: Biointerfaces 83 (2011) 155.
[36] A.B. Albadarin, C. Mangwandi, A.H. Al-Muhtaseb, G.M. Walker, S.J. Allen, M.N.M. Ahmad, Chemical Engineering Journal 179 (2012) 193.
[37] K.M.S. Sumathi, S. Mahimairaja, R. Naidu, Bioresource Technology 96 (2005) 309.
[38] Y.Y. Chang, J.W. Lim, J.K. Yang, Journal of Industrial and Engineering Chemistry 18 (2012) 188.